The Plant Cell, Vol. 7, 1951–1962, November 1995

Identification, Characterization, and Purification of a Tobacco Endonuclease Activity Induced upon Hypersensitive Response Cell Death

Ron Mittler and Eric Lam[1]

Center for Agricultural Molecular Biology, Cook College, P.O. Box 231, Rutgers, The State University of New Jersey, New Brunswick, New Jersey 08903-0231

Programmed cell death (pcd) is activated during the hypersensitive response (HR) of plants to avirulent pathogens. We have recently shown that, similar to pcd in animal cells, nuclei of cells undergoing HR cell death contain fragmented nuclear DNA (nDNA). Here, we report that cell death occurring during the HR is accompanied by an increase in the activity of several deoxyribonucleases. Induction of nuclease activities was coordinated with cell death and may account for the degradation of nDNA during the HR. HR-associated nuclease activities were not induced during senescence, following necrotic cell death resulting from abiotic stress, or in response to induction of plant defense mechanisms by salicylic acid. HR-associated nuclease activities were stimulated by Ca^{2+} and inhibited by EGTA, EDTA, and Zn^{2+}. At least one of the HR-associated nuclease activities was detected in nuclei purified from leaves undergoing pcd. A nuclease with an electrophoretic mobility similar to that of the nuclease activity found in nuclei isolated from leaves undergoing HR cell death was purified. Our findings are in accordance with some of the biochemical events that occur during pcd in animal cells. However, further analysis of the pattern of nDNA fragmentation and the corresponding structural changes that occur in the nuclei of tobacco cells undergoing HR cell death revealed that these features may have differences from those that take place during apoptosis in animal cells.

INTRODUCTION

Many incompatible plant–pathogen interactions result in the formation of hypersensitive response (HR) lesions and the activation of host defense mechanisms (Keen, 1990). During the HR, the recognition of a pathogen triggers the activation of a cell death pathway that results in the formation of a zone of dead cells around the infection site. This zone of dead cells is thought to function as a barrier that prevents further proliferation of the pathogen. Several lines of evidence suggest that death of host cells during the HR results from the activation of an intrinsic cell death program that is encoded by the plant genome. These lines of evidence stem from studies that demonstrate the activation of HR cell death by certain elicitors (Yang et al., 1993; Hammond-Kosack et al., 1994; Levine et al., 1994), by expression of different foreign genes (Takahashi et al., 1989; Becker et al., 1993; Mittler et al., 1995), and as a result of mutations in certain genes that are thought to be involved in the cell death pathway (Walbot et al., 1983; Wolter et al., 1993; Dietrich et al., 1994; Greenberg et al., 1994). In addition, HR cell death has been shown to require active plant metabolism and to depend on the activity of the host transcription and translation machinery (Yang et al., 1993; He et al., 1994). Therefore, cell death that occurs during the HR is not caused directly by the invading pathogen but rather results from activation of a host-encoded pathway for cell death. Hence, death of cells during the HR may be referred to as programmed cell death.

The term programmed cell death (pcd) is used to describe cell death that is a normal part of the life cycle of a multicellular organism. In animals, pcd is activated during the course of several developmental pathways and in response to certain viral pathogens and environmental stimuli (Schwartzman and Cidlowski, 1993; Vaux, 1993; Hacker and Vaux, 1994; Martin et al., 1994). One of the most widely studied forms of pcd is apoptosis, a type of pcd characterized by a distinct set of morphological and physiological features (Schwartzman and Cidlowski, 1993). A key characteristic of apoptosis is the systematic fragmentation and degradation of nuclear DNA (nDNA) that accompanies cell death (Wyllie et al., 1984; Bortner et al., 1995). Degradation of nDNA during apoptosis is coordinated with the activation of specific endonucleases that are thought to mediate chromatin cleavage (Schwartzman and Cidlowski, 1993). Degradation of nDNA during apoptosis is also believed to cause the condensation of nDNA and the fragmentation of the nuclei (Wyllie et al., 1984). However, not all cases of pcd in animal cells take the form of apoptosis (Schwartz et al., 1993).

We reported previously that HR-associated cell death and developmentally controlled pcd that occur during the maturation

[1] To whom correspondence should be addressed.

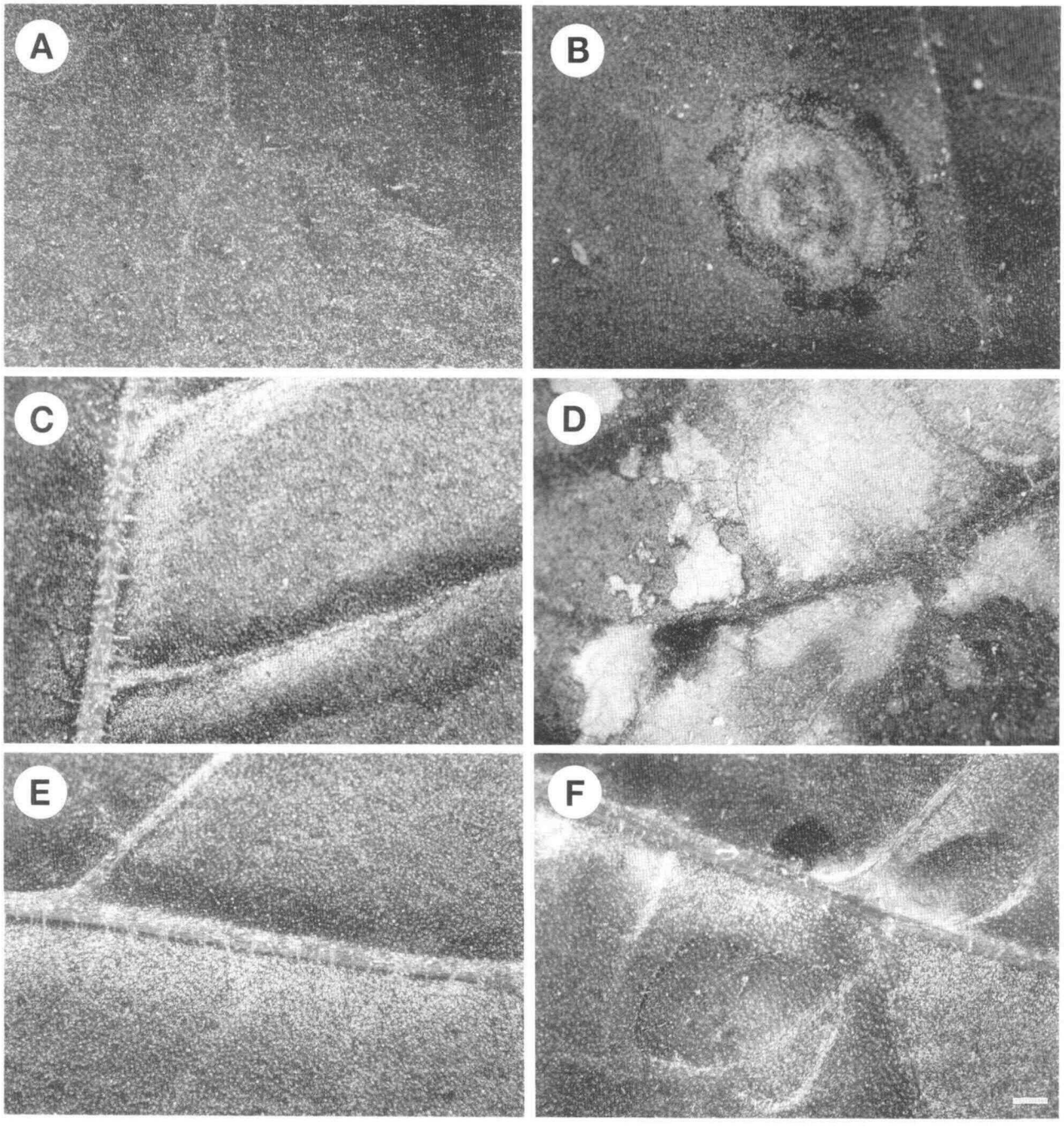

Figure 1. Activation of TMV-Induced and *bO*-Triggered Cell Death in Tobacco Plants.

(A) Mock-infected Xanthi-nc NN leaf.
(B) TMV-infected Xanthi-nc NN tobacco leaf showing the formation of an HR lesion 48 hr postinfection at 22°C.
(C) TMV-infected Samsun NN tobacco leaf grown at 30°C showing symptoms indicative of systemic TMV infection.
(D) Activation of the HR cell death pathway in systemically infected plants 72 hr following a temperature shift from 30 to 22°C.
(E) Leaf of a transgenic tobacco plant expressing the *bO* gene grown at 30°C showing no cell death.
(F) Formation of spontaneous lesions on a leaf of a *bO*-expressing plant 48 hr following a temperature shift from 30 to 22°C. Bar = 1 mm.
Plants were grown and infected with TMV as described in Methods.

of xylem elements involve the degradation of nDNA (Mittler and Lam, 1995; Mittler et al., 1995), one of the hallmarks of apoptosis in animal cells. Here, we demonstrate that activation of the HR in plants is accompanied by an increase in the activity of several deoxyribonucleases. At least one of these nucleases was detected in purified nuclei. This nuclease was purified from leaves undergoing HR cell death, and its endonucleolytic activity was directly demonstrated. Our findings suggest that induction of nuclease activity is correlated with activation of the HR cell death pathway in higher plants.

RESULTS

Activation of Pcd in Plants

The incompatible interaction between tobacco mosaic virus (TMV) and tobacco plants that contain the *N* gene results in the formation of HR lesions (Figures 1A and 1B). The formation of these HR lesions is inhibited at high temperature. Therefore, TMV-resistant cultivars can be systemically infected by TMV at 30°C (Figure 1C). Upon shifting of the infected plants from 30 to 22°C, the inhibition of HR cell death activation is removed and cell death occurs (Figure 1D; Whitham et al., 1994). Recently, we have shown that expression of the bacterial proton pump bacterio-opsin (bO) can lead to the formation of spontaneous lesions similar to those observed during the HR. This transgenically triggered pcd is also inhibited at 30°C (Figures 1E and 1F; Mittler et al., 1995). We have therefore utilized infection with TMV at 22°C (Figures 1A and 1B) as well as a temperature shift protocol (Figures 1C to 1F) for inducing HR cell death in tobacco. As shown in Figure 1, *bO*-expressing transgenic plants and TMV-infected wild-type plants developed very few or no lesions at 30°C (Figures 1C and 1E). However, upon shifting of these plants from 30 to 22°C, lesions developed within 48 hr (Figures 1D and 1F). Cell death was quantitated by measuring ion leakage from leaf discs obtained from mock- and TMV-infected plants at 22°C, from plants systemically infected with TMV at 30°C and shifted to 22°C, and from *bO*-expressing plants grown at 30°C and shifted to 22°C (Figure 2A). This relatively synchronized induction of cell death upon temperature shift from 30 to 22°C may thus serve as a useful experimental system for studying the different molecular events that occur during pcd in plants.

Nuclei of cells undergoing developmentally controlled and pathogen- or *bO*-triggered cell death contain fragmented nDNA (Mittler and Lam, 1995; Mittler et al., 1995). This finding indicates that at least some forms of cell death in plants involve an active process of nDNA degradation that may be similar to pcd or apoptosis in animal cells. Because some cases of pcd in animal cells are accompanied by induction of nuclease activity (Schwartzman and Cidlowski, 1993), we tested whether nuclease activity is also induced during HR-associated cell death in plants.

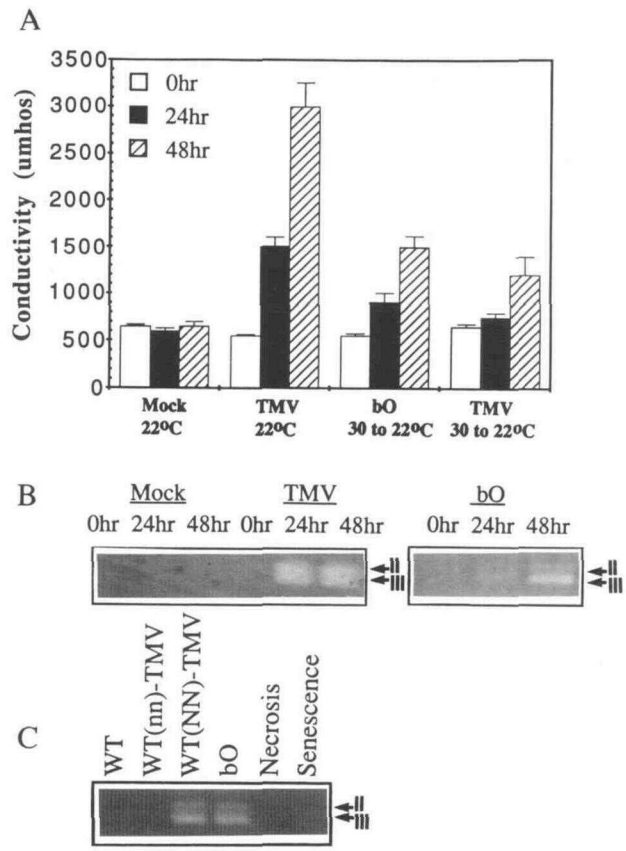

Figure 2. Induction of HR-Specific Nuclease Activities during Pathogen-Induced and Transgenically Triggered Cell Death.

(A) Ion leakage from leaf discs obtained from mock- and TMV-infected Xanthi-nc NN plants at 22°C and from TMV-infected and *bO*-expressing Samsun NN plants grown at 30°C and shifted to 22°C.

(B) Induction of nuclease activity in mock- and TMV-infected Xanthi-nc NN plants at 22°C (left) and in *bO*-expressing Samsun NN plants grown at 30°C and shifted to 22°C (right).

(C) Induction of nuclease activities in wild-type (WT) Samsun NN, wild-type Xanthi nn infected with TMV (WT(nn)-TMV), wild-type Samsun NN infected with TMV (WT(NN)-TMV), and *bO*-expressing Samsun NN (bO) plants 72 hr following a temperature shift from 30 to 22°C and in leaves undergoing necrotic cell death resulting from abiotic stress (2 hr following a freeze–thaw treatment; Necrosis) and senescing leaves (containing 10% of the chlorophyll content of fully expanded photosynthetically active leaves; Senescence).

Arrows in **(B)** and **(C)** indicate the different nucleases induced during activation of the HR-associated cell death (II and III represent NUCII and NUCIII, respectively). Ion leakage and nuclease activity were assayed as described in Methods. Conductivity is expressed in micromhos (umhos).

Induction of Nuclease Activity during HR-Associated Cell Death

The induction of nuclease activity during cell death in plants was studied with leaves obtained from mock- and TMV-infected

tobacco plants at 22°C, *bO*-expressing plants and TMV-infected wild-type plants following a temperature shift as described above, and *bO*-expressing plants and wild-type plants grown at 22°C. We have used a gel assay to detect nuclease activity in protein extracts obtained from plants undergoing cell death. This assay allowed us to correlate nuclease activity with a particular protein band. Activation of cell death was coordinated with induction of three putative nucleases (NUC): NUCI, 100.5 kD; NUCII, 38 kD; and NUCIII, 36 kD. Induction of NUCII and NUCIII activities was observed in TMV-infected plants at 22°C (Figure 2B, left). NUCII and NUCIII were also induced in *bO*-expressing and TMV-infected plants upon a temperature shift from 30 to 22°C (Figures 2B, right, and 2C). However, NUCI activity was detected only in TMV-infected and *bO*-expressing plants following a temperature shift (data not shown).

The induction of nuclease activities was tested at different time points following activation of HR cell death. Nuclease activities were only detected late during the cell death process (i.e., 24 to 72 hr postactivation of cell death). Fragmentation of nDNA was also detected at a similar time interval following activation of cell death, that is, 24 to 72 hr after cell death activation (data not shown; Mittler et al., 1995). Fragmentation of nDNA, as detected by the TUNEL assay, and induction of nuclease activity were not detected at 6 and 12 hr postactivation of cell death (data not shown). These results suggest that the process of pathogen-induced cell death in plants is accompanied in some cases by induction of nuclease activities and that these nuclease activities may account for the degradation of nDNA during or following this death process.

Induction of Pcd-Associated Nuclease Activities Is Linked with HR Cell Death

An increase in nuclease activity may also accompany cell death that occurs during senescence or following necrosis, which results from abiotic stress. The induction of nuclease activities was therefore examined in senescing leaves and in plants that underwent a freeze–thaw treatment (Figure 2C). No induction of HR-associated nuclease activities was found in senescing leaves or in samples obtained from leaves undergoing abiotically induced necrotic cell death (0.5, 2, or 8 hr following a freeze–thaw treatment). In addition, TMV-infected plants that did not contain the *N* gene, and therefore would not respond via HR cell death to TMV infection, exhibited no induction of nuclease activities (Figure 2C). These results further demonstrate the specificity of the induced nuclease activities to cell death associated with the HR.

During the HR, cell death is coordinated with the induction of a general defense mechanism that involves synthesis of pathogenesis-related (PR) proteins and accumulation of antimicrobial compounds called phytoalexins. To examine whether the induction of nuclease activity is a result of activating such a general defense mechanism or whether it is under the control of a distinct pathway, we treated wild-type plants with salicylic acid (SA). Treatment of tobacco plants with SA

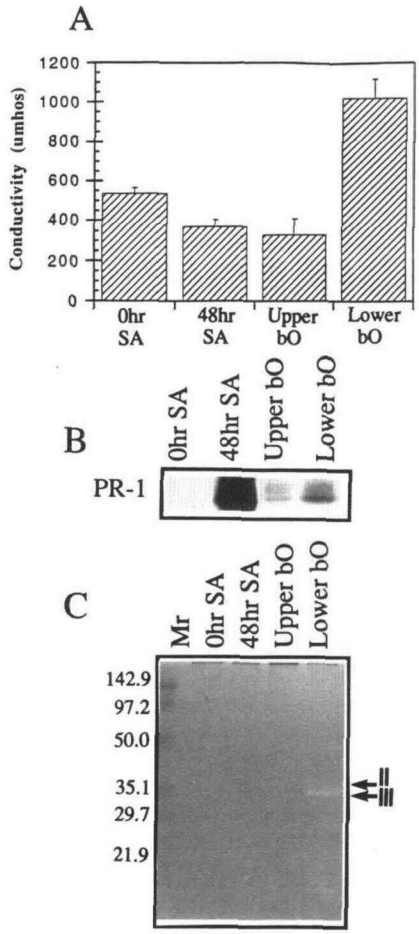

Figure 3. HR-Associated Nucleases Are Not Induced by SA.

(A) Ion leakage from leaf discs obtained from control (0 hr; SA) and SA-treated (48 hr; SA) Samsun NN plants and from upper and lower leaves of a transgenic Samsun NN plant expressing the *bO* gene. **(B)** and **(C)** Accumulation of PR-1a protein **(B)** and induction of nuclease activities **(C)** in protein extracts obtained from control and SA-treated and *bO*-expressing plants shown in **(A)**. Arrows in **(C)** indicate the major pcd-associated nucleases NUCII (top) and NUCIII (bottom). Wild-type tobacco plants were watered with 2 mM SA and sampled 48 hr following SA application. Upper and lower leaves of transgenic plants expressing the *bO* gene were used as controls. Upper leaves of *bO*-expressing plants contain high levels of SA and PR-1a protein but have no lesions, whereas lower leaves of these plants contain high levels of SA and PR-1a protein, and develop spontaneous lesions (Mittler et al., 1995). Cell death, PR-1a protein, and nuclease activity were assayed as described in Methods. Conductivity is expressed in micromhos (umhos). Molecular mass (Mr) markers are given at left in kilodaltons.

is known to result in the induction of PR proteins and the acquisition of systemic resistance (Ward et al., 1991). Tobacco plants treated with SA did not develop lesions (Figure 3A) and did not activate HR cell death–associated nuclease activities (Figure 3C). These plants did, however, accumulate PR-1a

protein (Figure 3B). This result indicates that the induction of nuclease activity is linked with activation of cell death and is independent of application of external SA or the production of the PR-1a protein.

Characterization of Pcd-Associated Nuclease Activities

NUCI, NUCII, and NUCIII were capable of degrading both single- and double-stranded DNA, as determined with the nuclease gel assay (data not shown). The effect of different divalent cations on the activity of the three pcd-associated nucleases was studied. As shown in Figure 4, the activity of these nucleases was inhibited by EGTA or EDTA. However, the activity of NUCI could be restored by the addition of either Ca^{2+} or Mg^{2+}, whereas the activity of NUCIII was more specific and could only be restored by Ca^{2+}. The inhibition of NUCII could not be restored by either Ca^{2+} or Mg^{2+}. We also tested the effects of Mn^{2+}, Cu^{2+}, and Fe^{2+} on restoring NUCII and NUCIII activities in the presence of EGTA or EDTA. None of these ions was able to restore NUCII and NUCIII activities under these conditions (data not shown). Because pcd-associated nuclease activity in animals is inhibited by Zn^{2+} (Schwartzman and Cidlowski, 1993; Peitsch et al., 1994), we tested the effect of Zn^{2+} on the activity of the three nucleases. Zn^{2+} at a concentration of 1 mM was found to inhibit the activity of all three nucleases (Figure 4). However, the presence of 10 μM Zn^{2+} had no effect on the activity of these nucleases (data not shown).

A pcd-associated nuclease (NUC 18) has been found in the nuclei of thymocytes undergoing glucocorticoid-induced pcd (Compton and Cidlowski, 1987; Gaido and Cidlowski, 1991). We therefore tested whether any of the pcd-associated nucleases are found in the nuclei of cells undergoing pcd. As shown in Figure 5, some NUCIII activity was found in nuclei purified from leaves undergoing pcd. Because nuclear extracts may contain high levels of histone activity that can be detected as apparent nuclease activity by staining DNA-containing gels (Gaido and Cidlowski, 1991), we performed the nuclease assay with gels that contained ^{32}P-labeled DNA as a substrate (Figure 5C). As shown in Figure 5C, NUCII and NUCIII activities were detected as a region of degraded substrate DNA (a band with no radiolabeled DNA), whereas the presence of histones is indicated by regions of condensed radiolabled DNA (Figure 5C).

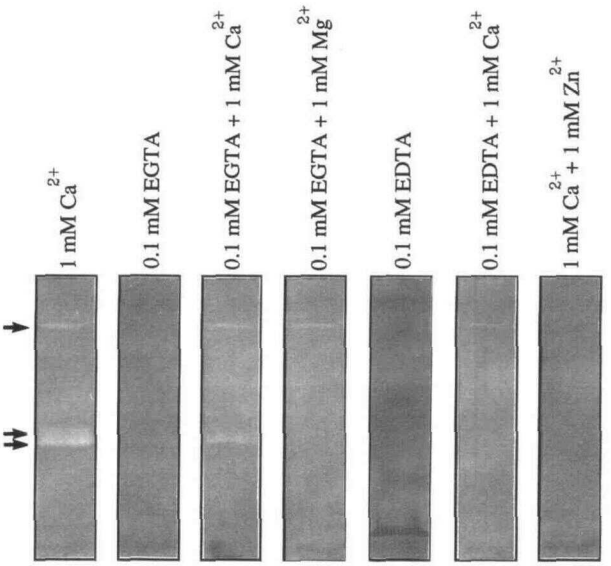

Figure 4. Inhibition of HR-Associated Nuclease Activities by EGTA, EDTA, and Zn^{2+}.

Protein extracts obtained from TMV-infected wild-type plants 72 hr following a temperature shift from 30 to 22°C were analyzed for nuclease activities as described in Methods, except that gels were washed and incubated in 10 mM Mops, pH 6.8, 20 μM $CaCl_2$, and 10 μM $MgCl_2$ containing the various inhibitors and cations as indicated. Arrows indicate the major pcd-associated nucleases (top, NUCI; middle, NUCII; bottom, NUCIII).

Purification and Characterization of NUCIII: A Pcd-Associated Endonuclease

To characterize further the nucleolytic properties of the pcd-associated nucleases, we purified the nuclease activity that corresponded to NUCIII on our nuclease gel assays (Figure 6). NUCIII activity was thermostable and could be recovered from the supernatant following heat denaturation at 95°C and slow renaturation at room temperature (described in Methods). This step proved to be an effective purification step. Further purification was achieved by an ammonium sulfate precipitation (60 to 95%), ion exchange chromatography, and affinity chromatography on a concanavalin A column. The binding of NUCIII activity to concanavalin A may indicate that this nuclease is a glycoprotein. Finally, NUCIII activity was purified to apparent homogeneity by hydroxyapatite chromatography followed by either SDS–polyacrylamide gel or gel filtration with a Superdex 75 column. A silver-stained SDS of the final preparation revealed a single band with an apparent molecular mass of 34.5 kD (Figure 6B). Interestingly, the mobility of NUCIII on an activity gel corresponded to an apparent molecular mass of 36 kD (Figure 6C).

To confirm that the protein band detected by the silver-stained SDS–polyacrylamide gel corresponded to the activity found in the nuclease gel assay, the 34.5-kD protein was cut out of the gel, eluted, and subjected to the nuclease gel assay. The nuclease activity detected with this gel assay showed that the purified 34.5-kD protein indeed corresponds to NUCIII (Figure 6C). This finding suggests that the electrophoretic mobility of NUCIII may be affected by the presence of single-stranded DNA and/or fibrinogen in the activity gel.

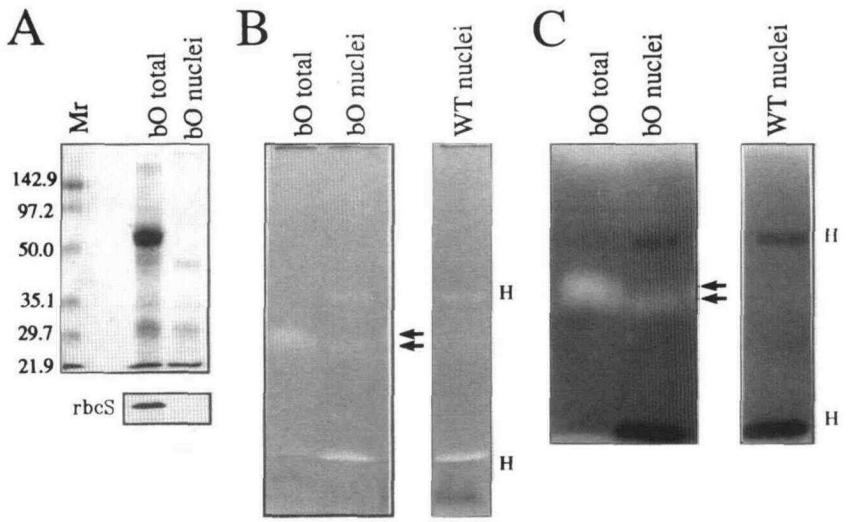

Figure 5. Occurrence of an HR-Associated Nuclease Activity (NUCIII) in Purified Nuclei.

(A) Protein gel stained with Coomassie blue (top) and immunoblot probed with an antibody raised against the small subunit of ribulose-1,5-bisphosphate carboxylase (RbcS) (bottom) showing the absence of contaminating chloroplastic proteins in protein extracts from purified nuclei.
(B) and **(C)** Nuclease activities in protein extracts obtained from purified nuclei of wild-type (WT) and lesion-containing transgenic plants expressing the *bO* gene (bO). Nuclease activity was assayed by staining DNA-containing gels with toluidine blue **(B)** or by incorporating ^{32}P-labeled substrate DNA into the gels **(C)**, as described in Methods. Arrows indicate NUCII (top arrow) and NUCIII (bottom arrow); H, putative histone activity. Nuclei were purified on Percoll gradients as described in Methods. Molecular mass (Mr) markers are given at left in kilodaltons.

To examine the nucleolytic properties of NUCIII, the protein purified via gel filtration was incubated with denatured salmon sperm DNA and supercoiled plasmid DNA. Following incubation at 45°C, the digested DNA was analyzed on agarose gels. The NUCIII protein was capable of degrading both single-stranded salmon sperm DNA and double-stranded plasmid DNA (Figures 7A and 7B). NUCIII was also capable of degrading purified tobacco DNA (data not shown). Degradation of circular, supercoiled plasmid DNA indicates that NUCIII is an endonuclease. NUCIII attacks the DNA molecule by first nicking the DNA on one strand to form a relaxed (nicked) plasmid (Figure 7B). Further nicking of the DNA molecule results in the linearization of plasmid DNA (Figure 7B) and subsequent degradation.

Mechanism of nDNA Degradation during HR-Associated Cell Death

In animals, pcd is often associated with morphological and physiological changes known as apoptosis. A unique feature of this process is the systematic fragmentation and degradation of nDNA. Large fragments of 300 and 50 kb are first produced by endonucleolytic degradation of higher order chromatin. These fragments are further degraded by cleavage at linker DNA sites between nucleosomes (Wyllie et al., 1984; Walker et al., 1993), resulting in DNA fragments that are multimers of ~180 bp. These can be detected by agarose gels as a "DNA ladder" (Schwartzman and Cidlowski, 1993). However, the degradation of nDNA during pcd in animal cells may also occur via a different process that does not result in DNA ladders (Schwartz et al., 1993).

Nuclei of tobacco cells undergoing HR cell death contain fragmented nDNA (Mittler et al., 1995). It is unclear, however, whether the fragmented nDNA in these nuclei is the result of a systematic fragmentation process similar to apoptosis or the outcome of a different degradation process that may be similar to pcd processes that do not take the form of apoptosis. We therefore tested whether the degradation of nDNA during HR cell death involves a DNA-degrading mechanism that results in the formation of DNA ladders.

DNA isolated from leaves undergoing HR cell death in response to a TMV infection at 22°C (Figure 8A), from stems of *bO*-expressing plants shifted from 30 to 22°C (Figure 8B), and from TMV-infected wild-type plants grown at 30°C and shifted to 22°C (data not shown) was analyzed by electrophoresis on agarose gels. Although these DNA preparations contained degraded DNA, we could not observe any indication for the formation of DNA ladders upon activation of HR cell death (Figures 8A and 8B). To increase the sensitivity of this assay, we transferred the DNA to nylon membranes and hybridized them to a mixture of DNA probes (Figures 8D and 8E). This method increases the sensitivity of the assay for the detection of low molecular weight DNA fragments (Schwartz et al., 1993). However, we could not observe the formation of DNA ladders even with this method of detection (Figures 8D

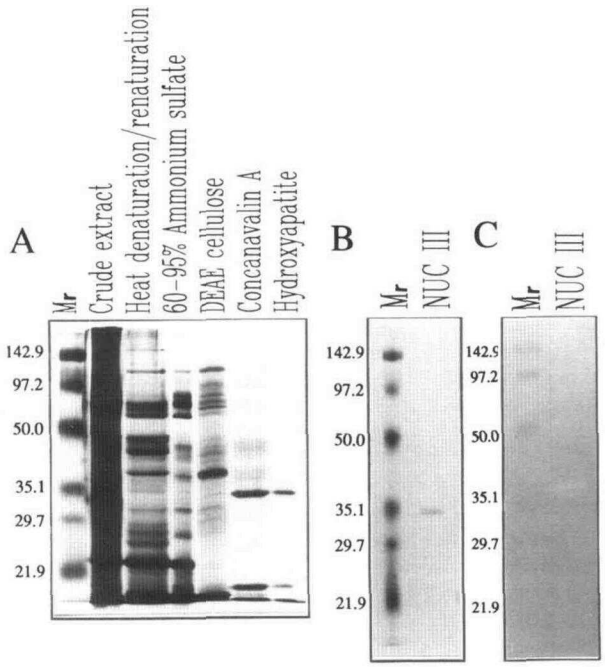

Figure 6. Purification of a Pcd-Associated Endonuclease (NUCIII).

(A) Silver-stained SDS–polyacrylamide gel (12% resolving gel) of different protein samples obtained during the purification of NUCIII. The different protein samples represent different purification steps as described in the text.

(B) Silver-stained SDS–polyacrylamide gel (12% resolving gel) of purified NUCIII.

(C) Nuclease gel assay of purified NUCIII. NUCIII was purified by SDS–polyacrylamide gel as shown in **(B)** and briefly stained with Coomassie blue. The 34.5-kD NUCIII protein band was cut out of the gel and ground to a powder. The NUCIII protein was eluted in 10% glycerol, 0.1% SDS, 50 mM Tris-HCl, pH 7, at 65°C for 30 min and subjected to the nuclease gel assay.

Silver staining and activity staining were performed as described in Methods. Molecular mass (Mr) markers are given at left in kilodaltons.

and 8E). As a positive control, we treated nDNA of isolated tobacco nuclei with micrococcal nuclease, an enzyme that digests nDNA preferentially at linker sites between nucleosomes. DNA from these nuclease-treated nuclei was isolated using the same DNA isolation protocol used for plant tissues undergoing HR cell death and subjected to electrophoresis on similar agarose gels. As shown in Figure 8C, DNA ladders could be detected clearly by electrophoresis on agarose gels. DNA ladders were also detected by hybridization of DNA blotted from these gels with the same mixture of probes that was used for the detection of DNA degradation in DNA isolated from plant tissues undergoing HR cell death (Figure 8F). As a control for random DNA degradation that presumably occurs during abiotically induced necrosis, we isolated DNA from wild-type leaves at 8 hr after a freeze–thaw treatment (Figures 8B and 8E). Two additional methods were used in an attempt to detect the formation of DNA ladders. DNA was isolated using the Hirt protocol (Lakshmi et al., 1992). This DNA, together with DNA shown in Figures 8D and 8E, was treated with the Klenow fragment of DNA polymerase I in the presence of ^{32}P-labeled dATP or dCTP and subjected to electrophoresis as described by Rosi (1992). No evidence for the formation of DNA ladders was observed (data not shown).

The systematic nDNA fragmentation that occurs during apoptosis in animal cells is thought to result in the collapse of chromatin structure, the condensation of nDNA, and the breakdown of the nuclei (Wyllie et al., 1984; Schwartzman and Cidlowski, 1993; Peitsch et al., 1994). The condensation and fragmentation of nuclear material in apoptotic nuclei can be easily observed by light microscopy (Martin et al., 1994). We have therefore examined whether nuclei of cells from tobacco stems undergoing HR cell death contain condensed nuclear material and whether these nuclei may form distinct nuclear debris by fragmentation. As shown in Figure 9, nuclei of plant cells undergoing HR cell death do not contain condensed nuclear material and do not appear to undergo fragmentation.

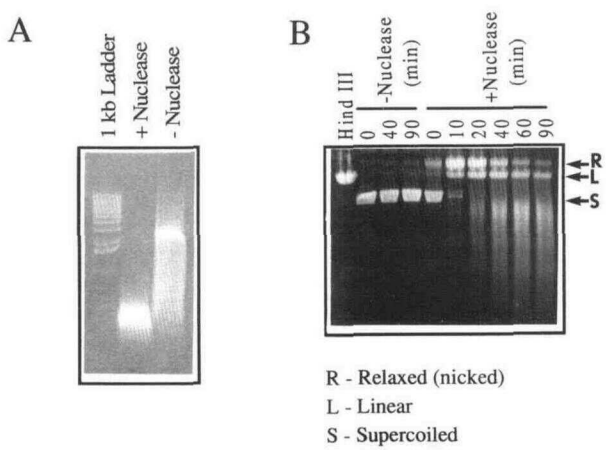

Figure 7. Digestion of Single-Stranded and Double-Stranded DNA Substrate by Purified NUCIII.

(A) Digestion of single-stranded salmon sperm DNA in solution. Heat-denatured salmon sperm DNA (6 μg) was incubated for 90 min at 45°C with (+) or without (−) 10 ng of purified NUCIII. After digestion, DNA was separated on a 1% agarose gel and stained with ethidium bromide.

(B) Digestion of double-stranded supercoiled plasmid DNA. Purified NUCIII (10 ng) was incubated with 10 μg of plasmid DNA (pSP64; Promega) at 45°C. At different time points, an aliquot was removed from the reaction and placed on ice. Plasmid DNA was also digested with the restriction endonuclease HindIII in a separate reaction to produce a linear form of the plasmid as a control. DNA digests were performed as described in Methods. After digestion, DNA was separated on a 1% agarose gel and stained with ethidium bromide. Molecular mass DNA standard fragments (Bethesda Research Laboratories; 1-kb ladder) were used to distinguish between digested (low molecular mass) and undigested single-stranded DNA.

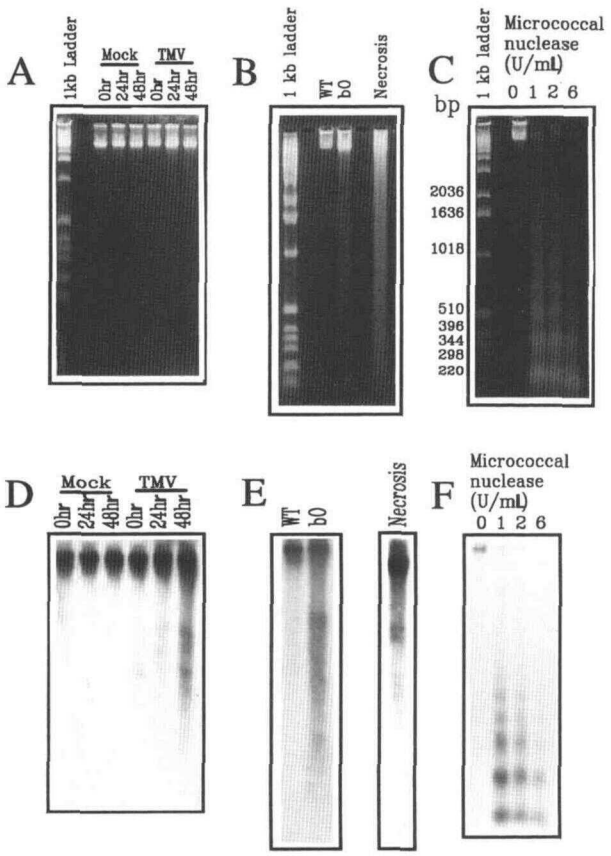

Figure 8. Detection of DNA Degradation during HR-Associated Cell Death.

(A) and **(B)** DNA isolated from mock- and TMV-infected Xanthi-nc NN plants **(A)**, from wild-type and *bO*-expressing plants 48 hr following a temperature shift from 30 to 22°C **(B)**, and from wild-type (WT) leaves undergoing necrotic cell death resulting from abiotic stress (Necrosis) **(B)**, was analyzed for the presence of DNA ladders by electrophoresis on 2% agarose gels and staining with ethidium bromide.

(C) Detection of DNA ladders in DNA isolated from wild-type tobacco nuclei digested with micrococcal nuclease. U, units.

(D) to **(F)** Gel blot analysis of DNA transferred from the gels shown in **(A)** to **(C)**, respectively, with a mixture of six probes for different tobacco genes. This method is expected to increase the sensitivity of the assay shown in **(A)** to **(C)** for the detection of DNA ladders (Schwartz et al., 1993).

DNA isolated from wild-type tobacco nuclei that were treated with micrococcal nuclease served as a positive control for the detection of DNA ladders. Sizes of the visible low molecular mass DNA standard fragments (Bethesda Research Laboratories; 1-kb ladder) are indicated in **(C)**. DNA isolation, gel blot analysis, and micrococcal nuclease digestion were performed as described in Methods.

These nuclei do, however, appear to contain regions of degraded nuclear material. Similar observations were reported previously for tobacco leaves undergoing HR cell death (Hayashi and Matsui, 1965; Graca and Martin, 1975). This observation correlates with the lack of an organized pattern of nDNA degradation (Figure 8) that is thought to cause condensed nuclear material during apoptosis (Wyllie et al., 1984). In contrast with the appearance of nuclei in cells undergoing HR cell death (Figures 8B and 8C), nuclei of cells undergoing necrotic cell death following a freeze–thaw treatment apparently lost their nuclear envelope and appeared very disorganized (Figure 8D). Loss of organized nuclear structure is a common feature in cells undergoing necrotic cell death (Schwartzman and Cidlowski, 1993).

DISCUSSION

In animal cells, pcd is associated with the induction of cellular mechanisms that participate in the dismantling process of the dying cell (Martin et al., 1994). These may include the activation of cell death–associated nucleases in the dying cell or in neighboring cells that engulf and degrade the debris produced by the dying cell (Peitsch et al., 1994). It is not clear at present whether nucleases are required for the cell death process or whether they are simply involved in removing the

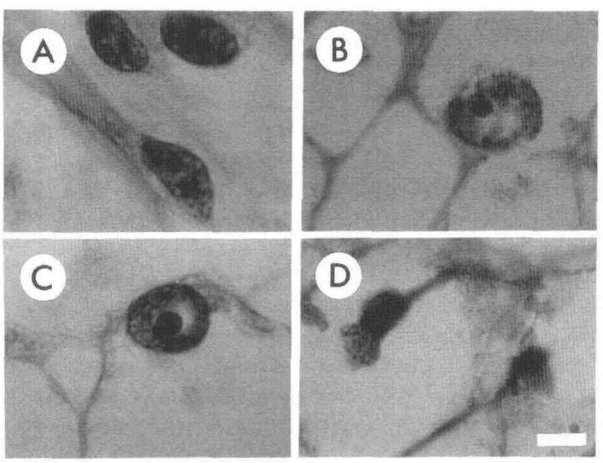

Figure 9. Nuclear Morphology in Cells Undergoing HR Cell Death and Abiotically Induced Cell Death.

(A) Nuclei of wild-type untreated tobacco plants.

(B) Nuclei of cells undergoing TMV-induced cell death (48 hr following a temperature shift from 30 to 22°C).

(C) Nuclei of cells undergoing *bO*-induced cell death (48 hr following a temperature shift from 30 to 22°C).

(D) Nuclei of cells undergoing necrotic cell death 10 min following a freeze–thaw treatment. Bar = 15 μm.

The structure of nuclei from wild-type plants grown at 30°C and from wild-type plants infected with TMV and grown at 30°C was similar to that of nuclei from untreated wild-type plants shown in **(A)** (data for mock- and TMV-infected plants grown at 30°C are not shown). Tobacco stems were sectioned midway between petiole–stem nodes and processed for histology as described in Methods.

contents of the dead cell. In some cases, inhibition of nDNA degradation was shown to prevent apoptosis, indicating that chromatin cleavage may represent a key step in this process (Schwartzman and Cidlowski, 1993). However, the degradation of nuclei from neuronal cells undergoing pcd during the development of *Caenorhabditis elegans* occurs only after the debris from the dying cell have been engulfed by the neighboring cells (Ellis and Horvitz, 1986). It is therefore possible that cell death may occur via distinct pathways that utilize nucleases in a different manner. Regardless of nucleases' active or passive role in mediating cell death, it is clear that nuclease activity is required for the removal of nDNA during or following cell death.

We have previously reported that nuclei of cells undergoing HR pcd contain fragmented nDNA (Mittler et al., 1995). This finding may indicate that degradation of nDNA is part of the HR cell death pathway. Here, we report that TMV-induced and *bO*-triggered cell death is accompanied by an increase in the activity of several deoxyribonucleases. Increased nuclease activity as well as nDNA degradation appeared to occur at a late stage during the cell death process (i.e., 24 hr postactivation of cell death) and were not detected at 6 and 12 hr postinduction of cell death. This may indicate that in the case of HR cell death in tobacco, the induced nuclease activity is not the direct cause of cell death but is rather a downstream event that is part of the HR cell death process. It is not clear at present whether the increase in nuclease activity reflects post-translational activation of preexisting nucleases or the de novo synthesis of new nucleases. Induction of nuclease activities did not occur during senescence or necrotic cell death resulting from a freeze–thaw treatment. In addition, TMV infection of tobacco plants that do not contain the *N* gene did not result in nuclease induction. Thus, the induced deoxyribonucleases appear to be specific for cell death associated with the HR. However, it is not known whether nuclease activity will also be induced in plant cells undergoing cell death that is caused by pathogen-produced toxins. In animal cells, toxin-induced cell death can apparently result from the activation of a pcd process (Chang et al., 1989). It is therefore possible that nuclease activity can also be induced during pathogen-derived cell death that does not involve the activation of the HR in plants.

NUCIII activity was purified to homogeneity, and its nucleolytic activity against single-stranded DNA and supercoiled plasmid DNA was confirmed (Figures 6 and 7). The binding of NUCIII to concanavalin A suggests that this nuclease may be a glycoprotein. Further characterization of the NUCIII protein, including production of antisera and immunological analysis, may shed more light on the role of this nuclease in mediating nDNA degradation during pcd in plants. It should be noted that although the purified NUCIII exhibits true nucleolytic activity and its induction is correlated with HR cell death, other nucleases not detectable by the gel assay may also contribute to the process of nDNA degradation during HR cell death. The activity of these nucleases may depend on association with other proteins or subunits and may therefore not be detected following SDS-PAGE. Alternatively, these nucleases may not be capable of refolding to their active form following separation on SDS-PAGE. Nevertheless, our findings provide the initial evidence for the existence of HR-associated nucleases that may participate in nDNA degradation during the HR cell death process in higher plants.

Plants are fundamentally different from animal cells in a number of ways, and it is very unlikely that a dying cell, or debris from a dying cell (such as apoptotic bodies in animals), will be engulfed by a neighboring plant cell. Such a process is very likely to be hindered by the cell wall. In addition, cell death that occurs during the HR is accompanied by an increase in ion leakage (Figures 2A and 3A; Mittler et al., 1995), whereas cell death that occurs during apoptosis in animals does not (Martin et al., 1994). This finding indicates that plant cells may undergo pcd via a different mechanism that does not involve the formation of apoptotic bodies and their engulfment by neighboring cells. Thus, plants may have developed alternative mechanisms for dismantling the nucleus of the dying cell. These may include activation of a nuclear-localized nuclease, such as NUCIII, or the secretion of nucleases by neighboring cells that may degrade the nucleus of the dying cell, or a coordinated function of these nucleases. Secretion of nucleases from plant cells was previously shown to occur during growth of cells in culture and by cells of the aleurone layer during germination of barley seed (Oleson et al., 1982; Brown and Ho, 1987; Thelen and Northcote, 1989), supporting the possible occurrence of such a process in plants.

The mode of nDNA degradation in tobacco cells undergoing HR cell death does not appear to involve DNA ladder formation. DNA ladders have been interpreted as an indication that DNA is being digested at linker sites between nucleosomes. However, if the proteins constituting the nucleosomes are degraded by specific or nonspecific proteases during or before the induction of nucleases, nucleosomal DNA ladders may not form and the DNA degradation pattern will be more random. Because nuclei of plant cells undergoing HR-associated cell death contain fragmented nDNA (Mittler et al., 1995), this DNA may be degraded through a process not identical to that in classic apoptosis in animal cells. Some cases of pcd in animals may also involve a DNA degradation pathway that does not result in DNA ladders (Schwartz et al., 1993). Additional studies are needed to resolve these possible mechanisms for nDNA degradation during pcd in both animals and plants.

METHODS

Plant Material and Virus Infection

Wild-type tobacco plants (*Nicotiana tabacum* cvs Samsun NN, Xanthi-nc NN, and Xanthi-nn) and transgenic plants (Samsun NN) expressing the bacterio-opsin (*bO*) gene (R_1 progenies of EL301A plants; Mittler et al., 1995) were grown under continuous light. Fully expanded young

leaves of wild-type plants were infected with equal amounts of tobacco mosaic virus (TMV) strain U1 in 5 mM potassium phosphate buffer, pH 7, or were mock infected with the same 5 mM phosphate buffer by gently rubbing the leaves with carborundum. Plants were kept at 22 or 30°C under continuous light. No lesions developed on mock-infected leaves of wild-type plants or TMV-infected Samsun NN plants grown at 30°C. At this temperature, very few spontaneous lesions were observed in transgenic tobacco plants expressing *bO*. The progression of lesion formation in *bO*-expressing and TMV-infected Samsun NN plants following a temperature shift from 30 to 22°C, and in Xanthi-nc NN plants infected with TMV at 22°C, was assayed by measuring ion leakage from leaf discs obtained at different time points following the temperature shift or the virus infection as previously described (Mittler et al., 1995). Necrotic cell death was induced by incubating leaves of wild-type plants at −20 or −70°C for 60 min and thawing these leaves at 22°C for 0.5, 2, or 8 hr. Plant material was collected at various time points and flash frozen in liquid nitrogen.

Extraction of Proteins for Analysis of Nuclease Activity

Soluble leaf proteins were extracted by grinding leaves to a fine powder in liquid nitrogen and dissolving the powder in a buffer containing 100 mM 2-(*N*-morpholino)propanesulfonic acid (Mops), pH 6.8, 5 mM ascorbate, 2 mM reduced glutathione, 1 mM $CaCl_2$, 1 mM $MgCl_2$, 0.5 mM phenylmethylsulfonyl fluoride (PMSF), and 10 μM $ZnCl_2$ or by grinding frozen leaf material with a mortar and pestle at 4°C in the same buffer. SDS and Tris-HCl, pH 6.8, were added to a final concentration of 1.5% and 150 mM, respectively, and protein extracts were heated to 37 or 95°C for 5 min and centrifuged for 5 min at 10,000*g*. Protein extracts were recovered from the supernatant, subjected to SDS-PAGE as previously described (Mittler et al., 1995), and stained with Coomassie Brilliant Blue R250 for the estimation of protein content.

Detection of Nuclease Activity

Protein extracts were subjected to SDS-PAGE in gels that contained single- or double-stranded DNA substrate (50 μg/mL heat-denatured or native salmon sperm DNA [Sigma]) and 50 μg/mL bovine fibrinogen as described by Thelen and Northcote (1989). Following electrophoresis, the gels were washed twice for a total of 30 min with 25% isopropanol, 10 mM Mops, pH 6.8, 1 mM $CaCl_2$, 1 mM $MgCl_2$, and 10 μM $ZnCl_2$ and twice for a total of 60 min with 10 mM Mops, pH 6.8, 1 mM $CaCl_2$, 1 mM $MgCl_2$, and 10 μM $ZnCl_2$. The gels were then incubated overnight at 37 or 45°C in a buffer containing 10 mM Mops, pH 6.8, 1 mM $CaCl_2$, 1 mM $MgCl_2$, and 10 μM $ZnCl_2$. The activity of the renatured nucleases was observed by staining the gels with 0.02% toluidine blue (Sigma) for 10 min followed by extensive washing in 10 mM Mops, pH 6.8. Nuclease activity was detected as an achromatic region (band) that does not stain with toluidine blue due to the absence of DNA substrate. Bio-Rad prestained low molecular mass markers were used to estimate the apparent size of the electrophoretically separated nucleases. For detection of nuclease activity with ^{32}P-labeled DNA, salmon sperm DNA (0.5 μg) was heat denatured, annealed to 0.1 μg of heat-denatured and sheared salmon sperm DNA (Sigma) for 10 min at 37°C, and labeled using reagents from a random primer labeling kit (U.S. Biochemical), with ^{32}P-dATP, using 0.5 units of the Klenow fragment of DNA polymerase I.

^{32}P-labeled DNA was purified with a TE MIDI SELECT-D G-50 column (5′ prime–3′ prime, Inc., Boulder, CO) and introduced into SDS–polyacrylamide gels before polymerization of the gels as described above. After electrophoresis, the gels were washed and incubated as described above. The gels were then dried and exposed to x-ray films. Nuclease activity was detected as a region (band) without ^{32}P-labeled DNA. Histone activity was detected as an intense band due to the binding of DNA to histones and the concentration of ^{32}P-labeled DNA.

DNA Isolation and Analysis

Leaves (2 g) were ground to a fine powder in liquid nitrogen and resuspended in 12 mL of 1% SDS, 0.25 M sucrose, 50 mM NaCl, 10 mM EDTA, 50 mM Tris-HCl, pH 8, 20 μg/mL DNase-free RNase A preheated to 60°C. After incubation at 60°C for 15 min, the DNA was purified by extraction with an equal volume of phenol:chloroform:isoamyl alcohol (25:24:1). Sodium acetate (pH 7) was added to a final concentration of 0.3 M, and DNA was purified by an additional extraction with phenol:chloroform:isoamyl alcohol (25:24:1). DNA was precipitated by addition of two volumes of ethanol and incubation at −20°C overnight. DNA was washed, resuspended, and subjected to electrophoresis on 2% agarose gels. Electrophoresis was performed for 16 hr at 2 V/cm. After electrophoresis, DNA was visualized by staining with ethidium bromide. DNA was also isolated by the Hirt DNA isolation protocol (Lakshmi et al., 1992) and subjected to electrophoresis on agarose gels as described above. DNA was transferred to a Duralose-UV membrane (Stratagene), and hybridization was performed using either QuickHyb (Stratagene) or Image (U.S. Biochemical) hybridization solutions as suggested by the manufacturer. A mixture of six probes corresponding to six different tobacco genes (pathogenesis-related protein gene 1a, the ATPase β subunit, the small subunit of ribulose bisphosphate/carboxylase, glutamine synthase, TGA-1a, and GT-1a) was used for hybridization. DNA probes were labeled with a random primer labeling kit (U.S. Biochemical) using ^{32}P-dATP.

Purification of Nuclei and Nuclease Analysis

Nuclei were purified on Percoll gradients as previously described (Mittler and Zilinskas, 1994). Protein extracts were obtained by resuspending the purified nuclei in 1.5% SDS, 150 mM Tris-HCl, pH 6.8, 100 mM Mops, pH 6.8, 5 mM ascorbate, 2 mM reduced glutathione, 1 mM $CaCl_2$, 1 mM $MgCl_2$, 0.5 mM PMSF, 10 μM $ZnCl_2$ and heating to 95°C for 5 min. Protein was recovered from the supernatant following centrifugation for 5 min at 10,000*g*. For digestion with micrococcal nuclease, nuclei (equivalent of 150 μg of DNA) were resuspended in a buffer containing 0.25 M sucrose, 20 mM Mops, pH 6.8, 10 mM NaCl, 2 mM $CaCl_2$, 2 mM $MgCl_2$ and 1 mM DTT and incubated at 37°C for 15 min with 0, 1, 2, and 6 units/mL micrococcal nuclease (Sigma). After digestion, SDS and EDTA were added to final concentrations of 1% and 10 mM, respectively. DNA was extracted using the same protocol used for isolation of DNA from plant tissues undergoing hypersensitive response (HR) cell death and subjected to electrophoresis on agarose gels as described above.

Purification of an Endonuclease from Leaves Undergoing HR-Associated Programmed Cell Death

Tissue homogenization, ammonium sulfate precipitation, and dialysis were performed at 4°C. All chromatography steps were performed

at room temperature. Tobacco (Samsun NN) shoots with spontaneous HR lesions (2 kg) from transgenic plants expressing the *bO* gene were homogenized with 4 L of ice-cold buffer containing 100 mM Mops, pH 6.8, 5 mM ascorbate, 2 mM reduced glutathione, 1 mM $CaCl_2$, 1 mM $MgCl_2$, 0.5 mM PMSF, and 10 μM $ZnCl_2$. After filtration through four layers of Miracloth (Calbiochem, La Jolla, CA), the homogenate was heated to 95°C for 15 min and allowed to cool slowly to room temperature for 35 to 40 min. After heat denaturation/renaturation, the homogenate was centrifuged for 15 min at 8000*g*, and the pellet was discarded. Ammonium sulfate was slowly added, with constant stirring to the supernatant to achieve 60% saturation at 4°C, and the resulting supernatant was stirred for an additional 1 hr at 4°C. The pellet obtained following centrifugation at 8000*g* for 15 min was discarded. The concentration of ammonium sulfate in the supernatant was then similarly brought to 95% saturation. The pellet resulting from centrifugation at 8000*g* for 30 min was resuspended in 10 mM Mops, pH 6.8, 1 mM reduced glutathione, 1 mM $CaCl_2$, 1 mM $MgCl_2$, 10 μM $ZnCl_2$ and dialyzed for 14 hr against the same buffer.

The dialysate was applied to a DEAE cellulose (Sigma) column equilibrated with the same buffer, and nuclease activity was eluted with 100 mM NaCl. The fractions containing nuclease activity were dialyzed for 14 hr against 100 mM Mops, pH 6.8, 1 mM reduced glutathione, 1 mM $CaCl_2$, 1 mM $MgCl_2$, 10 μM $ZnCl_2$. The dialysate was applied to a concanavalin A–Sepharose 4B (Sigma) column equilibrated with the same buffer, and nuclease activity was eluted with 1 M *N*-acetyl-D-glucosamine. The fraction containing nuclease activity was dialyzed for 14 hr against 25 mM Tris-HCl, pH 6.8, 1 mM reduced glutathione, 0.5 mM $CaCl_2$, 0.1 mM $MgCl_2$, 10 μM $ZnCl_2$. The dialysate was applied to a Bio-Gel-HTP hydroxyapatite column (Bio-Rad) equilibrated with the same buffer, and nuclease activity was eluted with a step gradient of sodium phosphate buffer (10, 20, 40, 60, 80, and 100 mM). Nuclease activity was found in the 60 mM fraction. This fraction was concentrated by binding to a concanavalin A–Sepharose 4B column and elution with 1 M *N*-acetyl-D-glucosamine. The concentrated fraction was further concentrated with a Centriprep 3 filter (Amicon). This fraction contained two proteins, the purified nuclease and an additional 10-kD protein. The nuclease polypeptide was further purified to homogeneity by SDS-PAGE and assayed for nuclease activity with the nuclease gel assay. In addition, the concentrated hydroxyapatite 60 mM fraction was applied to a Superdex 75 column (Pharmacia) equilibrated with a buffer containing 100 mM Mops, pH 6.8, 1 mM $CaCl_2$, 1 mM $MgCl_2$, and 10 μM $ZnCl_2$, and the fractions containing the nuclease protein were assayed for nuclease activity by digesting single-stranded salmon sperm DNA or supercoiled plasmid DNA.

DNA digestions were performed in a buffer containing 100 mM Mops, pH 6.8, 1 mM $CaCl_2$, 1 mM $MgCl_2$, and 10 μM $ZnCl_2$ at 45°C. After incubation for various times, the digested DNA was subjected to electrophoresis on 1% agarose gels and visualized by staining with ethidium bromide. Silver staining was performed according to Rabilloud et al. (1988). This purification protocol yielded a total of 12 μg of pure nuclease. Similar results were obtained when this protocol was applied for the purification of nuclease activity from Xanthi-nc NN leaves undergoing HR programmed cell death in response to a TMV infection (data not shown).

Histochemistry and Microscopy

Tobacco stem sections (2 mm thick) were fixed in 10% formaldehyde–5% acetic acid–45% ethanol or 3% glutaraldehyde–0.1 M potassium phosphate, pH 7, for 3 hr, dehydrated through a graded ethanol series (25, 50, 75, and 100% for 20 min at each step), and incubated overnight in 100% ethanol (alternatively, tissue was stained with 0.5% eosin in 95% ethanol overnight and washed twice, 10 min each, in 100% ethanol). The dehydrated tissue was then taken through a graded xylene series (25, 50, 75, and 100% in ethanol for 1 hr at each step). Finally, the tissue was embedded in paraffin (Paraplast+; Fisher Scientific, Pittsburgh, PA) by a paraffin graded series (25, 50, 75, and 100% in xylene for 3 hr each step at 59°C). Tissues were infiltrated in 100% paraffin overnight at 59°C and sectioned with a Reichert-Jung 2040 retractable rotary microtome (Leica, Nussloch, Germany) at a thickness of 5 μm. Sections were mounted on slides, deparaffinized, and stained with hematoxylin (Fisher Scientific), according to the manufacturer's instructions, and observed by light microscopy with an optiphot microscope (EF-D; Nikon, Melville, NY).

ACKNOWLEDGMENTS

We thank Drs. Daniel Klessig and Gabrielle Tjaden for gifts of plasmids and antisera. We gratefully acknowledge Dr. Peter Day's critical comments. This work was supported in part by the New Jersey Commission of Science and Technology and the U.S. Department of Agriculture.

Received June 8, 1995; accepted August 31, 1995.

REFERENCES

Becker, F., Buschfeld, E., Schell, J., and Bachmair, A. (1993). Altered response to viral infection by tobacco plants perturbed in ubiquitin system. Plant J. **3,** 875–881.

Bortner, C.D., Oldenburg, N.B.E., and Cidlowski, J.A. (1995). The role of DNA fragmentation in apoptosis. Trends Cell Biol. **5,** 21–25.

Brown, P.H., and Ho, T.D. (1987). Biochemical properties and hormonal regulation of barley nuclease. Eur. J. Biochem. **168,** 357–364.

Chang, M.P., Bramhall, J., Graves, S., Bonavidas, B., and Wisnieski, B.J. (1989). Internucleosomal DNA cleavage precedes diphtheria toxin-induced cytolysis. J. Biol. Chem. **264,** 15261–15267.

Compton, M.M., and Cidlowski, J.A. (1987). Identification of a glucocorticoid-induced nuclease in thymocytes. J. Biol. Chem. **262,** 8288–8292.

Dietrich, R.A., Delaney, T.P., Uknes, S.J., Ward, E.R., Ryals, J.A., and Dangl, J.L. (1994). Arabidopsis mutants simulating disease resistance response. Cell **77,** 565–577.

Ellis, H.M., and Horvitz, R.H. (1986). Genetic control of programmed cell death in the nematode *C. elegans.* Cell **44,** 817–829.

Gaido, M.L., and Cidlowski, J.A. (1991). Identification, purification, and characterization of a calcium-dependent endonuclease (NUC 18) from apoptotic rat thymocytes. J. Biol. Chem. **266,** 18580–18585.

Graca, J.V., and Martin, M.M. (1975). Ultrastructural changes in tobacco mosaic virus–induced local lesions in *Nicotiana tabacum* L. cv. "Samsun NN." Physiol. Plant Pathol. **7,** 287–291.

Greenberg, J.T., Ailan, G., Klessig, D.F., and Ausubel, F.M. (1994). Programmed cell death in plants: A pathogen-triggered response

activated coordinately with multiple defense functions. Cell **77,** 551–563.

Hacker, G., and Vaux, D.L. (1994). Viral, worm and radical implications for apoptosis. Trends Biol. Sci. **19,** 99–100.

Hammond-Kosack, K.E., Harrison, K., and Jones, J.D.G. (1994). Developmentally regulated cell death on expression of the fungal avirulence gene *Avr9* in tomato seedlings carrying the disease-resistance gene *Cf-9*. Proc. Natl. Acad. Sci. USA **91,** 10445–10449.

Hayashi, T., and Matsui, C. (1965). Fine structure of lesion periphery produced by tobacco mosaic virus. Phytopathology **55,** 387–392.

He, S.Y., Bauer, D.W., Collmer, A., and Beer, S.V. (1994). Hypersensitive response elicited by *Erwinia amylovora* harpin requires active plant metabolism. Mol. Plant-Microbe Interact. **7,** 289–292.

Keen, N.T. (1990). Gene-for-gene complementarity in plant–pathogen interactions. Annu. Rev. Genet. **24,** 447–463.

Lakshmi, R., Debbas, M., Sabbatini, P., Hockenbery, D., Korsmeyer, S., and White, E. (1992). The adenovirus E1A proteins induce apoptosis, which is inhibited by the E1B 19kDa and Bcl-2 proteins. Proc. Natl. Acad. Sci. USA **89,** 7742–7746.

Levine, A., Tenhaken, R., Dixon, R., and Lamb, C. (1994). H_2O_2 from the oxidative burst orchestrates the plant hypersensitive disease resistance response. Cell **79,** 583–593.

Martin, J.S., Green, R.D., and Cotter, T.G. (1994). Dicing with death: Dissecting the components of the apoptosis machinery. Trends Biol. Sci. **19,** 26–30.

Mittler, R., and Lam, E. (1995). *In situ* detection of nDNA fragmentation during the differentiation of tracheary elements in higher plants. Plant Physiol. **108,** 489–493.

Mittler, R., and Zilinskas, B.A. (1994). Regulation of pea cytosolic ascorbate peroxidase and other antioxidant enzymes during the progression of drought stress and following recovery from drought. Plant J. **5,** 397–405.

Mittler, R., Shulaev, V., and Lam, E. (1995). Coordinated activation of programmed cell death and defense mechanisms in transgenic tobacco plants expressing a bacterial proton pump. Plant Cell **7,** 29–42.

Oleson, A.E., Janski, A.M., Fahrlander, P.D., and Wiesner, T.H. (1982). Nuclease I from suspension-cultured *Nicotiana tabacum*: Purification and properties of the extracellular enzyme. Arch. Biochem. Biophys. **216,** 223–233.

Peitsch, M.C., Georg, M., and Tschopp, J. (1994). The apoptosis endonucleases: Cleaning up after cell death. Trends Cell Biol. **4,** 37–41.

Rabilloud, T., Carpentier, G., and Tarroux, P. (1988). Improvement and simplification of low-background silver staining of proteins by using sodium dithionite. Electrophoresis **9,** 288–291.

Rosi, F. (1992). A simple and rapid method for the detection of apoptosis in human cells. Nucleic Acids Res. **20,** 5243.

Schwartz, L.M., Smith, S.W., Jones, M.E.E., and Osborne, B.A. (1993). Do all programmed cell death occur via apoptosis? Proc. Natl. Acad. Sci. USA **90,** 980–984.

Schwartzman, R.A., and Cidlowski, J.A. (1993). Apoptosis: The biochemistry and molecular biology of programmed cell death. Endocrine Rev. **14,** 133–151.

Takahashi, H., Shimamoto, K., and Ehara, Y. (1989). Cauliflower mosaic virus gene VI causes growth suppression, development of necrotic spots, and expression of defense-related genes in transgenic tobacco plants. Mol. Gen. Genet. **216,** 188–194.

Thelen, M.P., and Northcote, D.H. (1989). Identification and purification of a nuclease from *Zinnia elegans* L.: A potential molecular marker for xylogenesis. Planta **179,** 181–195.

Vaux, D.L. (1993). Toward an understanding of the molecular mechanisms of physiological cell death. Proc. Natl. Acad. Sci. USA **90,** 786–789.

Walbot, V., Hoisington, D.A., and Neuffer, M.G. (1983). Disease lesion mimic mutations. In Genetic Engineering of Plants, T. Kosuge and C. Meredith, eds (New York: Plenum Publishing), pp. 431–442.

Walker, P.R., Koklieva, L., LeBlanc, J., and Sikorska, M. (1993). Detection of the initial stages of DNA fragmentation in apoptosis. Biotechniques **15,** 1032–1040.

Ward, E.R., Uknes, S.J., Williams, S.C., Dincher, S.S., Wiederhold, D.L. Alexander, D.C., Ahl-Goy, P., Metraux, J.-P., and Ryals, J.A. (1991). Coordinate gene activity in response to agents that induce systemic acquired resistance. Plant Cell **3,** 1085–1094.

Whitham, S., Dinesh-Kumar, S.P., Choi, D., Hehl, R., Corr, C., and Baker, B. (1994). The product of the tobacco mosaic virus resistance gene N: Similarity to Toll and the interleukin-1 receptor. Cell **78,** 1101–1115.

Wolter, M., Hollricher, K., Salamini, F., and Schulze-Lefert, P. (1993). The *mlo* resistance alleles to powdery mildew infection in barley trigger a developmentally controlled defense mimic phenotype. Mol. Gen. Genet. **239,** 122–128.

Wyllie, A.H., Morris, R.G., Smith, A.L., and Dunlop, D. (1984). Chromatin cleavage in apoptosis: Association with condensed chromatin morphology and dependence on macromolecular synthesis. J. Pathol. **142,** 67–77.

Yang, H.S., Huang, H.C., and Collmer, A. (1993). *Pseudomonas syringae* pv. *syringae* Harpin: A protein that is secreted via the Hrp pathway and elicits the hypersensitive response in plants. Cell **73,** 1255–1266.